Cell, Vol. 75, 13–23, October 8, 1993, Copyright © 1993 by Cell Press

Brain Myosin-V Is a Two-Headed Unconventional Myosin with Motor Activity

Richard E. Cheney,* Maura K. O'Shea,*
John E. Heuser,† Milton V. Coelho,‡
Joseph S. Wolenski,* Enilza M. Espreafico,*‡
Paul Forscher,* Roy E. Larson,‡
and Mark S. Mooseker*
*Department of Biology
Yale University
New Haven, Connecticut 06511
†Department of Cell Biology
Washington University School of Medicine
St. Louis, Missouri 63110
‡Department of Biochemistry
School of Medicine at Ribeirão Preto
University of São Paulo
Ribeirão Preto
São Paulo 14049
Brazil

Summary

Chicken myosin-V is a member of a recently recognized class of myosins distinct from both the myosins-I and the myosins-II. We report here the purification, electron microscopic visualization, and motor properties of a protein of this class. Myosin-V molecules consist of two heads attached to an ~30 nm stalk that ends in a globular region of unknown function. Myosin-V binds to and decorates F-actin, has actin-activated magnesium-ATPase activity, and is a barbed-end-directed motor capable of moving actin filaments at rates of up to 400 nm/s. Myosin-V does not form filaments. Each myosin-V heavy chain is associated with approximately four calmodulin light chains as well as two less abundant proteins of 23 and 17 kd.

Introduction

A novel division of the myosin superfamily of molecular motors has recently been identified based upon sequencing studies of the yeast *MYO2* gene (Johnston et al., 1991), the mouse *dilute* coat color gene (Mercer et al., 1991), and a calmodulin-binding protein from vertebrate brain (the p190–calmodulin complex, now called myosin-V; Larson et al., 1988; Espreafico et al., 1992). These proteins contain a myosin-like head domain sharing ~40% sequence identity with the head domains of the conventional myosins-II, but are clearly distinct from the myosins-II and the myosins-I, based both on their predicted structural features and on phylogenetic analyses (Espreafico et al., 1992; Cheney et al., 1993; Goodson and Spudich, 1993). All members of this recently discovered class are characterized by the presence of an unusual neck domain containing six tandem repeats of a putative calmodulin/light chain–binding motif that we refer to as an IQ motif (Cheney and Mooseker, 1992; Espreafico et al., 1992). In addition, each of these proteins is predicted to contain a coiled-coil stalk followed by a presumably globular tail domain of unknown function. Although these proteins appear to constitute a widely distributed and phylogenetically ancient division of the myosin superfamily, relatively little is known about their properties.

Molecular genetic analyses of *dilute* and *MYO2* have led to suggestions that this class of myosins may be involved in membrane trafficking or targeting. The phenotype resulting from a mutation in the essential *MYO2* gene includes a failure to complete budding, a disorganized actin cytoskeleton, and an accumulation of vesicles (Johnston et al., 1991). Surprisingly, this *myo2* phenotype can be suppressed by the overexpression of a novel member of the kinesin superfamily of microtubule-based motors (Lillie and Brown, 1992), indicating some form of interaction between actin-based and microtubule-based transport systems. Mice lacking a functional *dilute* gene product suffer from seizures and die within a few weeks of birth (Silvers, 1979). *dilute* mice also exhibit a lightening of their coat color due to a defect in the transfer of melanosomes from the melanocytes, which synthesize these organelles, to the surrounding cells of a growing hair (Silvers, 1979). Because chicken myosin-V and the mouse *dilute* gene product share 91% overall sequence identity, myosin-V and dilute are likely to be functional homologs of one another (Espreafico et al., 1992). The immunofluorescence localization of myosin-V indicates that it is present at the tips of cellular processes and that it colocalizes with intracellular membranes in the perinuclear region (Espreafico et al., 1992).

Myosin-V was originally identified as a 190 kd calmodulin-binding protein present in actomyosin preparations from vertebrate brain (Larson et al., 1988, 1990). Like brush border myosin-I, the p190–calmodulin complex was found to have the unusual property of binding to its calmodulin light chains in the absence of calcium (Espindola et al., 1992). The calmodulin-binding sites were mapped to the region containing the six IQ motifs (Espreafico et al., 1992). In addition, p190 was shown to be a substrate for the calcium-dependent protease calpain, to be immunologically distinct from myosin-II, and to undergo phosphorylation by a calmodulin-dependent protein kinase (Larson et al., 1990; Espindola et al., 1992). Most importantly, the p190–calmodulin complex was shown to have ATPase activity, suggesting that this protein might function as a molecular motor (Espindola et al., 1992). We report here the characterization of highly purified myosin-V. We demonstrate that myosin-V is a molecular motor and that its activity appears to be regulated by Ca^{2+} concentrations in the physiological range. Electron microscopy indicates that myosin-V is a two-headed myosin that does not form filaments. The structure of myosin-V is remarkable for its extended neck domain containing the six IQ motifs; the organization of this region may have implications for the structure and regulation of all myosins.

Results

Purification of Myosin-V

Following the protocol outlined below, ~0.5 mg of highly purified myosin-V could be obtained from ~80 g of chick brain (Figure 1). The resulting preparations of purified myosin-V exhibited no evidence of contamination with other proteins, such as myosin-II, on heavily loaded gels (Figure 1, lane n). Myosin-V was soluble in low and high salt buffers at pH 7.2 and was concentrated to 100–200 μg/ml with no evidence of precipitation or filament formation.

Myosin-V Contains Multiple Light Chains

The presence of six IQ domains in the neck of myosin-V suggested that each heavy chain of this protein might contain binding sites for as many as six light chains. Based on scanning densitometry of several different preparations of myosin-V (using calmodulin and skeletal muscle myosin-II as standards), we measured 4.0 ± 0.7 mol of calmodulin per mole of myosin-V heavy chain. In addition to calmodulin, heavily loaded gels of purified myosin-V always revealed two additional but less heavily stained bands with apparent molecular masses of 23 and 17 kd (Figure 2). Like the calmodulin light chains, these proteins copurified with myosin-V during gel filtration and anion exchange chromatography and also cosedimented with myosin-V under a variety of other conditions (see below). The electrophoretic mobilities of the 23 kd and the 17 kd bands were distinct from those of calmodulin, which migrates at 21 kd in the absence of Ca^{2+} and at 16 kd in the presence of Ca^{2+} (Burgess et al., 1980). The 23 and 17 kd bands did not exhibit either the Ca^{2+}-dependent mobility shift or the solubility after boiling that are characteristic properties of calmodulin (Figure 2). When approximately equal amounts of the 23 kd, 17 kd, and calmodulin bands were loaded on gels and immunoblotted with the anti-calmodulin monoclonal antibody 1F11 (Hulen et al., 1991), only the calmodulin band was stained (data not shown).

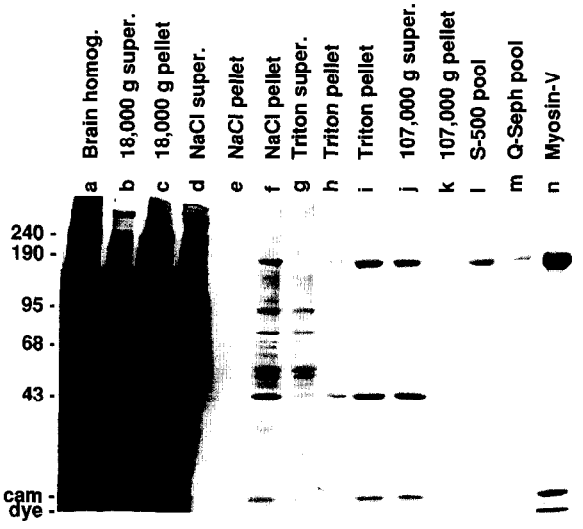

Figure 1. Purification of Myosin-V

Samples from the purification of brain myosin-V were analyzed by SDS–PAGE and Coomassie blue staining. Equal fractions based on percent volume were loaded in lanes a–e; lanes f–h were loaded 10 times more heavily and lanes i–m were loaded 33 times more heavily than lanes a–e. Lane n contains a 3 μg sample of purified myosin-V. The faint bands visible slightly below 190 kd are breakdown products that accumulate during storage. The mobilities of molecular mass standards in kilodaltons and calmodulin (cam) are indicated at left. Homog., homogenate; Super., supernatant; Seph, Sepharose.

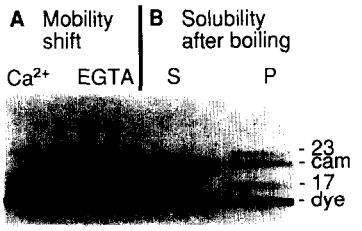

Figure 2. Characteristics of the Myosin-V Light Chains

Samples of the purified myosin-V illustrated in lane n of Figure 1 were analyzed by SDS–PAGE, and the low molecular mass region of the Coomassie-stained gel was enlarged to illustrate the myosin-V light chains. Note that in addition to the heavily stained calmodulin (cam) band, there are additional bands at 23 and 17 kd.

(A) The 23 and 17 kd bands do not exhibit the calcium-dependent mobility shift observed for the calmodulin light chains. Each lane was loaded with 3 μg of myosin-V in SDS–polyacrylamide gel sample buffer containing either 2 mM $CaCl_2$ or 2 mM EGTA as indicated.

(B) The 23 and 17 kd bands precipitate after boiling while the calmodulin remains soluble. A sample of myosin-V at 260 μg/ml in buffer A containing 1 mM EGTA was heated for 5 min at 100°C and centrifuged for 10 min at 105,000 × g in an airfuge, and equal fractions of the supernatant (S) and pellet (P) were loaded.

Visualization of Myosin-V by Electron Microscopy

Myosin-V molecules were visualized by electron microscopy after absorption on mica using the quick-freeze, deep-etch technique and rotary shadowing with platinum (Heuser, 1983). The micrographs clearly show that the myosin-V molecules contain two head domains (Figure 3; see Figure 4A). As noted below, the head domains visualized here probably consist of both the head and the neck domains defined by previous sequence analyses (Espreafico et al., 1992). The total length of a single myosin-V head and neck is 31 ± 3 nm. The two neck domains join at a thin stalk that extends for 30 ± 3 nm. This stalk typically ends in a small globule that is connected by a segment of variable length to a larger terminal globule. The variable segment appears to be flexible and can fold down onto the mica substrate in a variety of configurations. In some molecules, the larger and the smaller globules are superimposed. In others, the tail components have a maximal length of ~75 nm. In three-dimensional views of myosin-V (Figure 3), the distal ~10 nm of the head–neck region frequently appears to curl upward off of the mica substrate, much like the fingers of a boxing glove. This region also appears to be slightly thicker than the proximal ~20 nm, which has a relatively uniform thickness and probably corresponds to the neck domain. The 31 ± 3 nm length of the myosin-V head and neck is substantially longer than the 18 ± 3 nm we observed for head and

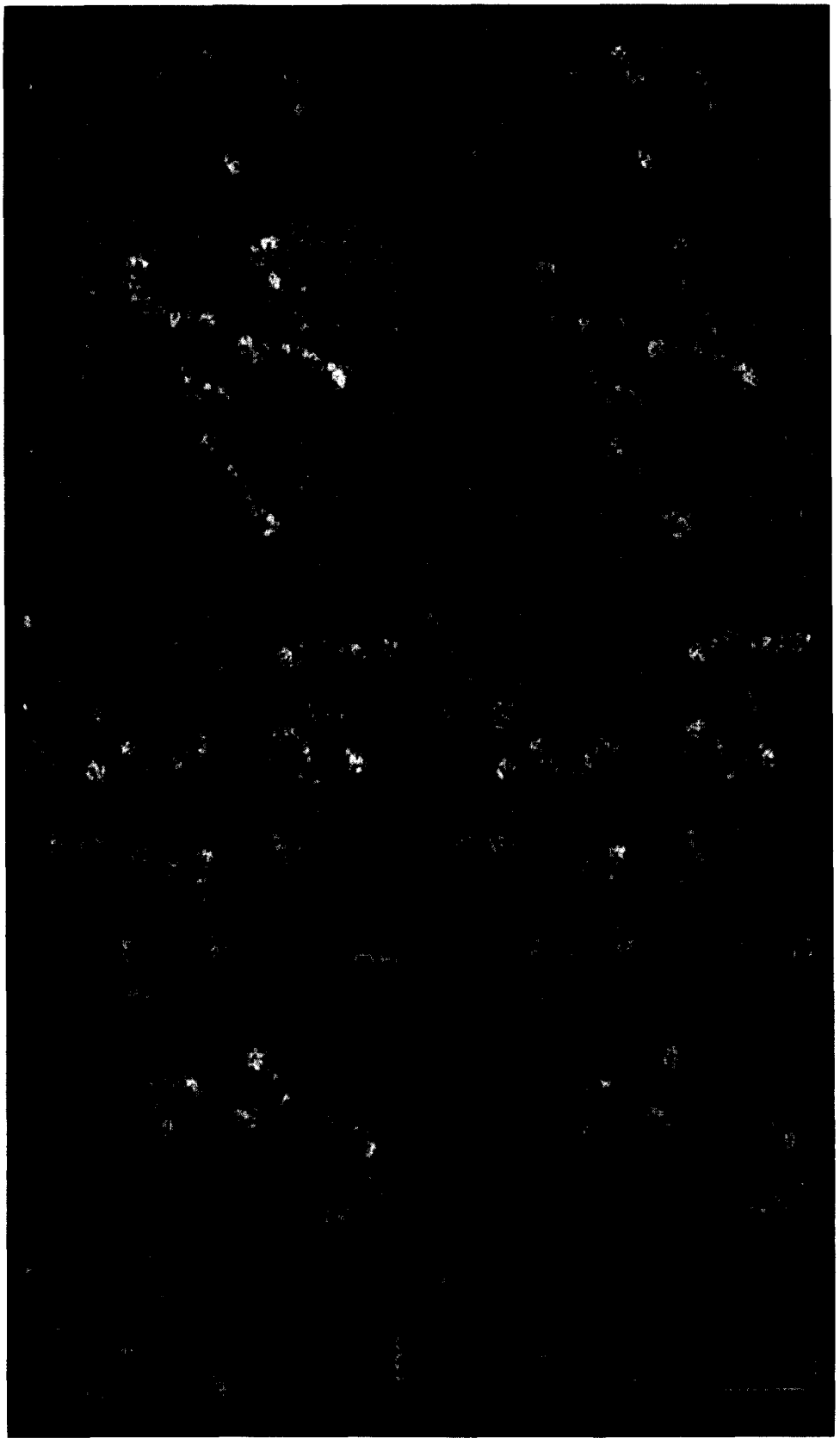

Figure 3. Stereo Pairs of Myosin-V Molecules Adsorbed on Mica and Visualized by Quick-Freeze, Deep-Etch Electron Microscopy

The upper stereo pair shows a single myosin-V molecule, while three molecules are visible in the next lower pair. Note that the myosin-V molecules have two unusually large head–neck domains attached to an ~30 nm stalk. The stalk appears to end in a small globule that is separated by a flexible segment from a larger globule at the end of the tail. Viewing these micrographs as stereo images greatly facilitates visualization of the myosin-V molecules through enhancement of their three-dimensional structure against the mica background below them. Scale bar, 50 nm.

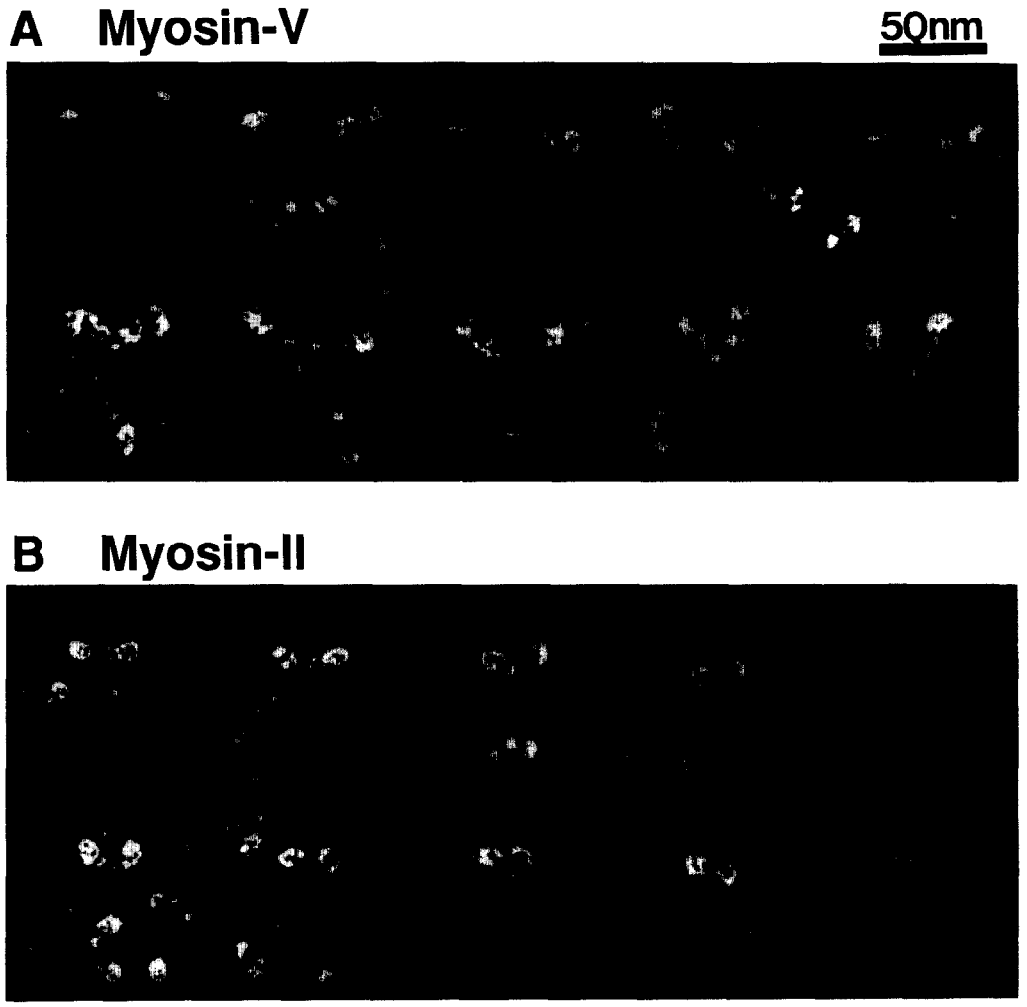

Figure 4. A Comparison of Myosin-V and Myosin-II Molecules Visualized on Mica by Quick-Freeze, Deep-Etch Electron Microscopy

(A) A gallery of myosin-V molecules. (B) A gallery of myosin-II molecules from A. castellani illustrating the head–neck region. Note that the head–neck domain of myosin-V is much longer in myosin-V than in myosin-II.

neck of conventional myosin-II molecules visualized by the same technique (compare Figures 4A and 4B).

Myosin-V Binds to and Decorates Actin Filaments

The interaction of myosin-V with actin filaments was examined by several techniques, including high speed cosedimentation and electron microscopic visualization of mixtures of myosin-V and actin. Like other myosins, myosin-V and its light chains cosedimented with F-actin in an ATP-inhibitable fashion (data not shown). When F-actin and myosin-V were mixed together in an ~1:1 molar ratio in the absence of ATP and visualized by negative staining, the characteristic arrowhead decoration of actin filaments was observed, demonstrating that myosin-V can bind to actin filaments in a fashion similar to other myosins (Figure 5A). Interestingly, many of the actin filaments in such preparations were cross-linked together into antiparallel arrays by myosin-V. Adjacent filaments in such arrays were spaced ~27 nm apart. This antiparallel cross-linking may be due to the presence of two heads on myosin-V, which are often held at 180° and can span 60–70 nm. In lightly stained regions (Figure 5B), the actin filaments decorated with myosin-V had a lampbrush appearance, with small strands radiating off for a distance of ~50 nm. Sometimes these strands appeared to end in globules. No evidence for the formation of myosin filaments (such as those formed by myosin-II) was observed either in these experiments or in the quick-frozen, deep-etched experiments. In addition to demonstrating that myosin-V could bind to actin, we also tested its ability to bind to microtubules using a cosedimentation assay. No cosedimentation of purified myosin-V with taxol-stabilized microtubules was observed in either the presence or absence of ATP (data not shown).

Myosin-V Is an Actin-Activated Magnesium-ATPase That Is Stimulated by Calcium

One of the defining properties of a myosin is its ability to hydrolyze ATP. It was thus important to determine whether purified myosin-V expressed the physiologically relevant actin-activated magnesium–ATPase activity expected of

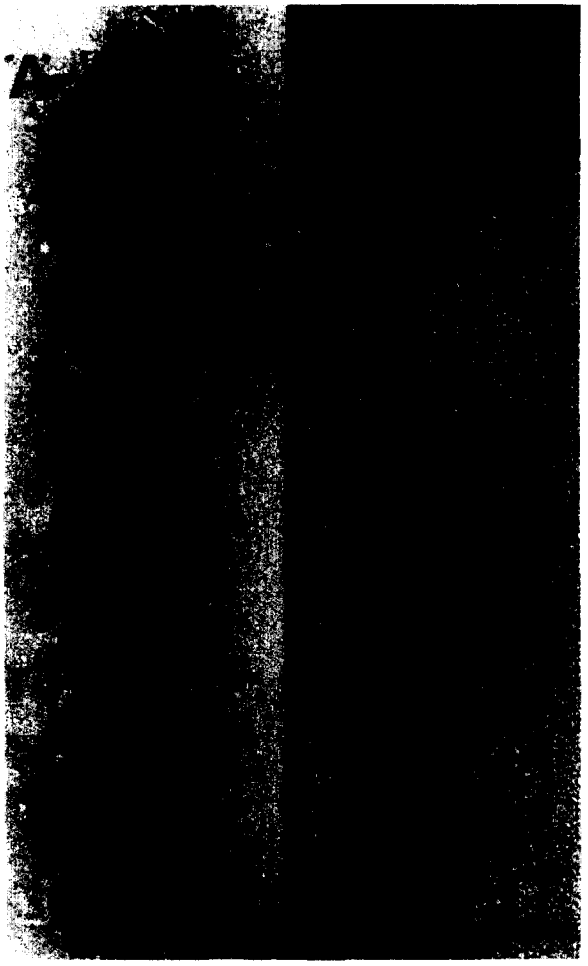

Figure 5. Negatively Stained Electron Micrographs of Myosin-V Bound to and Decorating Actin Filaments

(A) A bundle of actin filaments exhibiting clear arrowhead-type decoration with myosin-V. Note that the center filament has its barbed end oriented upward while the adjacent filaments have the opposite orientation.

(B) A more lightly stained field of actin filaments decorated with myosin-V at the same magnification. Note that faint strands can be seen radiating off of the actin filaments. Scale bar, 100 nm.

a myosin. In addition, since myosin-V contains multiple calmodulin light chains, we sought to determine whether the activity of myosin-V was regulated by micromolar concentrations of free Ca^{2+}. In the absence of actin, myosin-V had virtually no magnesium–ATPase activity in buffers containing either EGTA or 10 μM Ca^{2+} (Table 1). In the presence of actin and EGTA, the magnesium–ATPase activity was stimulated to relatively modest levels. In the presence of actin and 10 μM Ca^{2+}, however, the magnesium–ATPase activity was stimulated more than 100-fold to ~900 nmol of inorganic phosphate per milligram per minute (Table 1). Similar results were obtained from each of the three different myosin-V preparations tested.

Since some of the calmodulin light chains of myosin-V might have been lost after the addition of Ca^{2+} or during purification, the effect of exogenous calmodulin on the magnesium–ATPase activity of myosin-V was also examined (Table 1). Adding 25 μM calmodulin had little or no effect except when myosin-V, actin, and Ca^{2+} were all present; under these conditions, exogenous calmodulin further stimulated actin-activated magnesium–ATPase of myosin-V from 20%–56% in different experiments.

Table 1. Myosin-V Exhibits an Actin-Activated Magnesium–ATPase That Is Greatly Stimulated by 10 μm of Calcium

Condition	ATPase Activity[a]
Myosin-V plus EGTA	5
Myosin-V plus EGTA plus actin	127
Myosin-V plus EGTA plus actin plus calmodulin	148
Myosin-V plus Ca^{2+}	5
Myosin-V plus Ca^{2+} plus actin	920
Myosin-V plus Ca^{2+} plus actin plus calmodulin	1102

Samples contained myosin-V at 33 μg/ml in the presence or absence of 1110 μg/ml actin and 430 μg/ml calmodulin as indicated and were incubated for 30 min at 37°C. The ATPase buffer consisted of 27 mM imidazole, 26 mM KCl, 5.9 mM $MgCl_2$, 2.7 mM DTT, 2 mM ATP at pH 7.2 in the presence of either 1 mM EGTA or a 4 mM EGTA–calcium buffer calculated to generate a free calcium concentration of 10 μM. Conditions not shown, such as myosin-V plus calmodulin and calmodulin plus actin, had magnesium–ATPase activities of less than 10 nmol of inorganic phosphate per microgram per minute.

[a] Nanomoles of inorganic phosphate per milligram per minute.

Myosin-V Is a Barbed-End-Directed Molecular Motor

The mechanochemical activity of myosin-V was assessed using the sliding filament assay of Kron and Spudich (1986). Under optimal conditions of low Ca^{2+} (see below), actin filaments moved on myosin-V-coated coverslips at rates of ~300 nm/s (Figure 6A). Under these conditions, a constant rate of movement was observed for several hours. No movement occurred if either ATP or myosin-V was absent. Long actin filaments were usually sheared into smaller fragments in these motility assays. Solutions containing as little as ~1 μg/ml of myosin-V could support motility when adsorbed to the nitrocellulose-coated coverslips.

To determine the direction of myosin-V movement along actin filaments, myosin-V-coated beads were pipetted onto the actin cables of dissected Nitella cells. The myosin-V-coated beads moved in the same direction as beads coated with skeletal muscle myosin. This indicates that, like all other known myosins, myosin-V moves toward the barbed end of the actin filament. Myosin-V-coated beads moved at 29 ± 15 nm/s in the Nitella assay, which was much slower than the ~300 nm/s observed in the sliding filament assay. A similar disparity in rates between the two assays has been observed for brush border myosin-I (Wolenski et al., 1993a).

The In Vitro Motility of Myosin-V Is Inhibited by Calcium

Given that calcium greatly stimulated the actin-activated magnesium–ATPase activity of myosin-V, it was surprising to discover that calcium inhibited the activity of myosin-V in motility assays. When motility chambers were

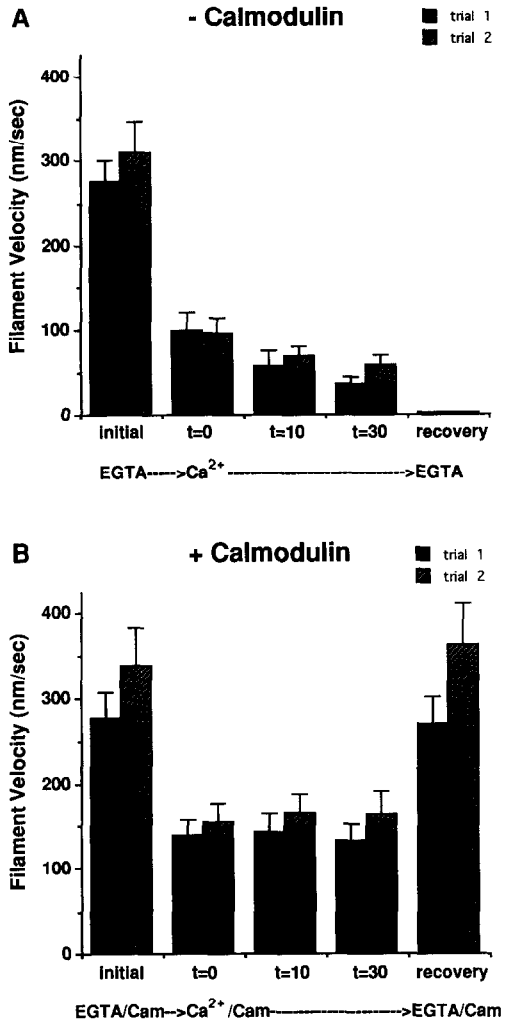

Figure 6. Myosin-V Translocates Actin Filaments in a Sliding Filament Motility Assay

(A) The effect of calcium on the rate of myosin-V-powered actin movement. The rate of filament movement on a myosin-V-coated coverslip was measured in motility buffer containing 1 mM EGTA, and then at timepoint 0 (t = 0), the chamber was switched to motility buffer containing 10 μM free calcium. Rate determinations were made immediately after the switch to calcium and after 10 and 30 min in calcium. After the 30 min timepoint, the chamber was returned to motility buffer containing 1 mM EGTA. The bars indicate the average filament velocities and their standard deviations. The closed and the hatched bars indicate data from two different experiments. Note that the addition of calcium causes an immediate drop in velocity that is followed by a gradual decay that does not recover when the chamber is returned to EGTA.

(B) The effect of calcium on the rate of myosin-V-powered actin movement when exogenous calmodulin (Cam) is present. The same protocol as in (A) was followed except that 300 μg/ml exogenous calmodulin was present in all of the motility buffer solutions. Note that the gradual decay in the rate of movement has been eliminated and that the rate recovers to normal upon return to EGTA.

switched from motility buffer containing EGTA to motility buffer containing 10 μM free Ca^{2+}, we observed an immediate decline in filament velocity to approximately half the initial value (Figure 6A). This apparently instantaneous drop in filament velocity occurred within the few seconds required to flush the new buffer into a chamber and refocus the microscope. With increasing time in 10 μM Ca^{2+}, a further but more gradual decline in the rate of movement was observed. This is illustrated in Figure 6A: after 30 min in Ca^{2+}, very few filaments were moving, and their rate of movement had declined to 10%–20% of the original value. When chambers were returned to motility buffer containing 1 mM EGTA after 30 min in Ca^{2+}, there was no recovery of movement. Ca^{2+} thus had two effects on the rates measured in the motility assay, an immediate inhibition that occurred within seconds and a gradual decay or inactivation that occurred over the course of ~30 min.

When the same type of experiment was performed in the presence of 300 μg/ml exogenous calmodulin, a different result was obtained (Figure 6B). Under these conditions, there was still an immediate drop in filament velocity when the chambers were switched from EGTA to Ca^{2+}, but there was no gradual decline in velocity during the 30 min incubation in Ca^{2+}. Furthermore, upon return to EGTA, the rates of movement recovered to their original levels. Adding exogenous calmodulin had no effect on filament velocity when EGTA was present. Thus, the chief effect of adding exogenous calmodulin was the elimination of the gradual inactivation caused by Ca^{2+}.

The importance of the calmodulin light chains for motility was demonstrated by use of the calmodulin antagonist W-7. When filaments moving in motility buffer containing EGTA were switched to motility buffer containing Ca^{2+} and 100 μM W-7, all movement immediately stopped and the filaments appeared to be tightly bound to the substrate (data not shown). As expected for an inhibitor that binds to calmodulin only in the presence of Ca^{2+}, W-7 had no effect on the rate of movement powered by myosin-V in EGTA.

Discussion

The results reported here demonstrate that myosin-V is in fact a myosin with properties distinct from both the conventional myosins-II and the myosins-I. These results also define several of the key structural and biochemical properties of this member of the myosin-V/dilute family.

A surprising feature of the myosin-V heavy chain is its relative abundance in brain, where we estimate from immunoblots that it constitutes ~0.3% of total protein. Thus, myosin-V is approximately as abundant as two other well-characterized motor proteins from brain, conventional myosin-II (~0.5% total brain protein; Burridge and Bray, 1975) and kinesin (~0.3% total brain protein; Hollenbeck, 1989). At this abundance, myosin-V would be expected to be a major calmodulin-binding protein of brain. It is interesting to note that a substantial fraction (27%) of the calmodulin in brain cortex is in fact reported to be resistant to extraction by EGTA (Kakiuchi et al., 1982). Calmodulin-binding sites that can bind in the absence of calcium, like those provided by the IQ motifs in proteins such as myosin-V, may also help to explain the very surprising result of Geiser et al. (1991) that the genetically essential functions of calmodulin do not require it to be able to bind calcium.

Light Chain Composition

A striking feature of the class V myosins is the presence of a neck domain consisting of six tandem repeats of a putative binding site for calmodulin or other proteins (or both) of the EF-hand superfamily (IQ motifs; Cheney and Mooseker, 1992; Espreafico et al., 1992). All reported myosins appear to contain at least one such motif in their neck domains. IQ motifs are frequently associated with the unusual property of binding to calmodulin in the absence of Ca^{2+}. In some cases Ca^{2+} actually leads to the release of calmodulin by these sites (Andreasen et al., 1983; Collins et al., 1990; Swanljung-Collins and Collins, 1991), which is exactly the opposite of the behavior expected for a conventional Ca^{2+}-dependent calmodulin-binding site.

Using gel scanning, we have measured a stoichiometry of 4.0 ± 0.7 calmodulin light chains per myosin-V heavy chain. In addition, we have identified two less abundant bands of 23 and 17 kd that cofractionate with myosin-V and appear to represent additional myosin-V light chains. This conclusion is also supported by preliminary cosedimentation experiments with liposomes, which indicate that myosin-V can bind to acidic phospholipids such as phosphatidylglycerol and that the 23 and 17 kd bands, like calmodulin, cosediment with the myosin-V heavy chain under these conditions. Based on preliminary gel scanning comparisons using the calmodulin light chains as standards, we estimate that the stoichiometry of the 23 and 17 kd bands is ~0.3:~0.7:1 relative to the myosin-V heavy chain. Although the 23 and 17 kd bands appear to be distinct from calmodulin, we have not ruled out the formal possibility that the 23 and 17 kd bands represent posttranslationally modified forms of calmodulin such as proteolyzed calmodulin or phosphocalmodulin. Phosphocalmodulin, for instance, does not undergo a Ca^{2+}-dependent mobility shift and has a molecular mass similar to that of the 17 kd protein (Plancke and Lazarides, 1983).

The light chain stoichiometry results reported here are consistent with the expectation from the presence of six IQ motifs that myosin-V contains multiple light chains, perhaps as many as six per heavy chain. In the future it will be important to determine the precise stoichiometry of the light chains, as well as the exact identity and nature of the 23 and 17 kd proteins. A key question is whether all of the myosin-V light chains bind to the IQ motifs in the neck domain or whether some of them, like the kinesin light chains, bind to the tail domain. It will also be important to determine whether all of the IQ motifs are equivalent or whether they are ordered in some way with respect to properties such as light chain affinity, calcium sensitivity, and regulatory function.

Structure of the Myosin-V Molecule

In general, the electron micrographs of myosin-V graphically confirm the predictions of myosin-V structure based on sequence data, and we have combined this information to generate the model of myosin-V structure shown in Figure 7. The distal ~10 nm of the myosin-V head–neck region, which appears similar in size and shape to the myosin-II head domain, almost certainly corresponds to the myosin-V head domain as defined by previous structure

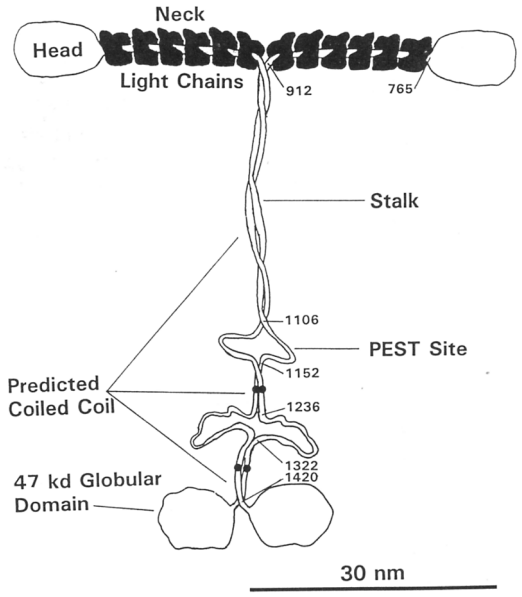

Figure 7. A Hypothetical Model of Myosin-V Structure Based on Its Primary Structure and Images from Electron Microscopy

Although six light chains (in black) are shown associated with the six IQ motifs in the neck domain, the precise number and disposition of the myosin-V light chains remain unknown. The location of the PEST sequence is also indicated. The numbers indicate the estimated positions of the amino acid residues corresponding to the beginning of the neck domain (amino acid 765) and the boundaries of the three major segments predicted to form coiled coils (amino acids 912–1106, 1152–1236, and 1322–1420). The closed circles within the latter two segments denote possible hinge regions.

predictions (Espreafico et al., 1992). The slightly narrower ~20 nm long region that connects the myosin-V head to the stalk region would thus correspond to the 18 kd neck domain consisting of the six IQ motifs (amino acids 765–909) and their associated light chains. If the six IQ motifs of the myosin-V neck bind to 6 light chains, a myosin-V dimer would contain 12 light chains. This would be consistent with the relatively large size of the neck seen in the micrographs of myosin-V.

The 30 nm stalk of the myosin-V molecule probably corresponds approximately to residues 912–1106 of the myosin-V heavy chain, which were predicted to form a largely uninterrupted segment of coiled-coil α helix (Espreafico et al., 1992). Such a 195 amino acid segment would form a coiled coil 29.0 nm in length; this is in close agreement with the observed length of the stalk of 30 ± 3 nm. It is likely that coiled-coil formation by this region leads the myosin-V heavy chains to dimerize.

The small globule observed at the end of the stalk and the segment of variable appearance may correspond roughly to residues 1107–1420 of the myosin-V heavy chain. This 36 kd region was predicted to have a mixed structure consisting of 5 kd domain containing a PEST sequence, a 12.6 nm segment of coiled coil, a 9 kd domain of unknown function, and a 13.4 nm segment of coiled coil (Espreafico et al., 1992; Figure 7). Although the function of this region is unknown, PEST sequences are frequently

associated with cleavage by the Ca^{2+}-dependent protease calpain (Wang et al., 1989). The presence of several segments of putative coiled coil may allow this region to fold down onto the mica in a variety of different configurations.

The large globule observed at the end of the myosin-V tail probably corresponds approximately to the carboxy-terminal 47 kd domain of myosin-V (amino acids 1421–1830). The primary structure of this region is highly conserved, exhibiting 97% amino acid sequence identity between chicken myosin-V and mouse dilute. This region does not share sequence similarity with either the putative actin-binding or membrane-binding sites present in the tail domains of the ameboid myosins-I. Although the function of this myosin-V tail domain is unknown, it may be involved in directing myosin-V to its targets or in determining its cargo. It is interesting to note that cleavage of myosin-V at or near the PEST site would cut the motor domain free from the globular tail.

The Myosin Neck Domain

The head and neck region of myosin-V is ~31 nm in length, which is much longer than the ~18 nm we observed for the corresponding region in myosin-II. The neck domain of the conventional myosin contains two IQ motifs (Espreafico et al., 1992; Cheney and Mooseker, 1992) in areas previously shown to be important for the binding of the essential and regulatory myosin light chains, and the myosin-II light chains, like calmodulin, are known to be members of the EF-hand superfamily of proteins. The striking difference in the length of the head–neck region between myosin-V and myosin-II is thus probably due to the four additional IQ motifs that are present in the neck domain of myosin-V. Although the actual structure formed by the IQ motifs in myosin-V is unknown, if the ~13 nm difference in length between the myosin-II and myosin-V heads is due to the presence of the four additional IQ motifs in the myosin-V neck, each IQ motif would be predicted to extend ~3.3 nm. This is close to the value of 3.6 nm that an ~24 amino acid IQ motif would span if it formed an α helix. In the recently determined structure of the myosin-II head, it is clear that the corresponding region of the myosin-II neck domain is in fact α helical (Rayment et al., 1993). The structure of calmodulin bound to a conventional Ca^{2+}-dependent calmodulin-binding site as revealed by nuclear magnetic resonance indicates that calmodulin can wrap around and clasp an α-helical calmodulin-binding site ~18–22 amino acids in length (Ikura et al., 1992). If the myosin-V calmodulin light chains were bound to the IQ motifs in a related fashion, the myosin-V neck would consist of an α-helical shaft ~20 nm long inserted into a sheath formed by six light chains. Such a structure suggests a large number of heavy chain motions that might be regulatable by the light chains.

In addition to the class V myosins, several other unconventional myosins appear to have extended neck domains. Brush border myosin-I, which binds to three to four calmodulin light chains (Hayden et al., 1990; Swanljung-Collins and Collins, 1991; Collins et al., 1990), has a neck that contains at least three IQ motifs, and the splice insert identified by Halsall and Hammer (1990) would add a fourth. A recently discovered myosin-I from vertebrate brain also contains four IQ motifs in its neck domain; the neck of this myosin undergoes alternative splicing that can lead to the insertion of up to two additional repeats (Ruppert et al., 1993). A recently reported and novel myosin from the higher plant Arabidopsis thaliana also contains an extended neck domain consisting of four IQ motifs (Knight and Kendrick-Jones, 1993). Thus, although all myosins appear to contain a neck domain with at least one IQ motif, the number of repeats (and thus the size of the neck) varies dramatically among different myosins and different splice forms of the same myosin.

ATPase Properties of Myosin-V

The defining and physiologically relevant ATPase activity for most myosins is an actin-activated magnesium–ATPase. We report here that myosin-V exhibits a modest actin-activated magnesium–ATPase activity that is greatly stimulated by micromolar concentrations of Ca^{2+}. In the absence of actin, myosin-V exhibited an ATPase activity of <0.1 ATP per second per molecule; the maximal level of activity that we observed in the presence of Ca^{2+}, actin, and exogenous calmodulin was ~14 ATP per second. This value is ~5–10 times greater than that reported for the initial myosin-V preparation (Espindola et al., 1992) and is similar to the ATPase activity of myosin-II from nonmuscle sources. The stimulatory effect of Ca^{2+} on the actin-activated magnesium–ATPase of myosin-V could result from either a direct regulatory effect of Ca^{2+} on myosin-V or from an indirect process such as Ca^{2+}-stimulated phosphorylation. Direct regulation by Ca^{2+} is known to occur in scallop muscle myosin-II (Kendrick-Jones and Scholey, 1981), where the light chains are believed to repress ATPase activity unless Ca^{2+} is bound. It is possible that a direct binding of Ca^{2+} to one or more of the myosin-V light chains performs a similar role.

The additional stimulation of the calcium- and actin-activated magnesium–ATPase of myosin-V observed when exogenous calmodulin is added may be due to a replenishment of calmodulin light chains lost during purification or during incubation with Ca^{2+}. Similar stimulatory effects of exogenous calmodulin have been observed with brush border myosin-I, in which early preparations did not include a full complement of light chains (Mooseker et al., 1991) and in which Ca^{2+} can cause the loss of enough calmodulin light chains that actin-activated magnesium–ATPase activity is inhibited (Swanljung-Collins and Collins, 1991).

Myosin-V Is a Molecular Motor

The clear conclusion from the sliding filament motility assay is that myosin-V is a motor protein capable of translocating actin filaments at rates of up to 200–400 nm/s. This is substantially faster than the 30–60 nm/s reported for brush border myosin-I (Mooseker et al., 1991), but slower than the 3000–4000 nm/s reported for muscle myosin-II (Kron and Spudich, 1986). A variety of intracellular movements occur at or slower than the rate of myosin-V-

powered movement, although caution should be used in extrapolating rate measurements from in vitro to in vivo conditions.

It is extremely unlikely that the motility observed here is due to contamination with another myosin, such as conventional myosin-II from brain. First, heavily loaded samples of myosin-V showed no evidence of contamination by other myosins when stained with Coomassie blue. Second, purified samples of myosin-V contained no detectable myosin-II by immunoblotting with a monoclonal antibody to human platelet nonmuscle myosin that clearly stained myosin-II in extracts of chicken brain (data not shown). Finally, myosin-V supported movement when absorbed at concentrations as low as ~1 μg/ml. If a contaminant were responsible for the motility, we estimate that it would be functioning at a concentration below ~1–10 ng/ml; this concentration is much lower than the ~5 μg/ml required for myosin-II-powered movement under similar conditions (Toyoshima et al., 1990).

Regulation of Myosin-V Activity by Calcium

The in vitro motility experiments also indicated that the motility of myosin-V can be regulated by calcium and calmodulin. The gradual decline in motility observed during incubations with Ca^{2+} and the observation that this decline could be prevented by the addition of exogenous calmodulin suggests that Ca^{2+} causes myosin-V to release calmodulin. Although unusual, such a loss of affinity for calmodulin in the presence of Ca^{2+} has been observed for several other proteins that contain IQ motifs, such as brush border myosin-I (Collins et al., 1990; Swanljung-Collins and Collins, 1991) and neuromodulin (Andreasen et al., 1983). The importance of calmodulin in the regulation of myosin-V is also indicated by the complete inhibition of motility observed in the presence of the calmodulin antagonist W-7.

Surprisingly, 10 μM Ca^{2+} inhibited movements powered by myosin-V in the motility assay, even though Ca^{2+} greatly stimulated the actin-activated magnesium–ATPase activity of myosin-V. A number of other researchers have also reported differences in behavior between ATPase and motility assays (Umemoto and Sellers, 1990; Takiguchi et al., 1990). There are several possible explanations for this phenomenon. Most simply, Ca^{2+} could lead to a decoupling of ATP hydrolysis from force production. It is also known that movement in motility assays can be dramatically inhibited by the "loads" imparted by contamination with as little as 1 part in 1000 of an actin-binding protein (Janson et al., 1992). The presence of subpopulations of tightly bound or more slowly moving motors might cause similar loading effects, and the numerous light chains of myosin-V raise the possibility of a very large number of different regulatory states for this myosin. Since Ca^{2+} appears to cause a dissociation of calmodulin from myosin-V, it is also possible that the myosin is artifactually inactivated under these conditions by the interaction of its "naked" and highly charged neck with the nitrocellulose substrate, as is suggested for brush border myosin-I in Wolenski et al. (1993b). Thus, although myosin-V exhibits regulation by physiological concentrations of Ca^{2+} in both the ATPase and the motility assays, it is currently unclear which assay better reflects the regulation of myosin-V activity within the cell.

Possible Roles of Myosin-V

At present the cellular functions of the proteins in this fifth class of the myosin superfamily are unknown. Although myosin-V may function primarily in the cell periphery as a component of a membrane or the cortical cytoskeleton, immunofluorescence studies indicate that much of the myosin-V in cells is associated with one or more of the membranous organelles that are located in the perinuclear region (Espreafico et al., 1992). If myosin-V is in fact associated with membranous organelles, it may function simply as a structural anchor or as a passenger on vesicles undergoing transport by microtubule-based motors. Alternatively, myosin-V may function as part of an actin-based transport system for organelles, as has been suggested by the recent results of Kuznetsov et al. (1992) with extruded squid axoplasm.

Experimental Procedures

Purification of Myosin-V

Approximately 80 chicks (1–7 days after hatching) were sacrificed by cervical dissociation, and their brains, including the cerebelli and brain stems, were rapidly removed (~70 g of brain total). All subsequent steps were performed at 4°C or on ice. Batches of 10 brains were placed in a 55 ml Potter-Elvehjem Teflon-on-glass homogenizer (Wheaton, Millville, New Jersey) and mixed with 50 ml of freshly prepared ice-cold 25 mM Tris–HCl, 10 mM potassium–EDTA, 0.3 mM phenylmethylsulfonyl fluoride, 0.1% β-mercaptoethanol, and 5 mM disodium ATP (the pH of this buffer was readjusted to 8.5 immediately after the addition of the solid ATP, using a pH meter standardized and operated at 0°C). The brains were homogenized by six up and down strokes of the Teflon pestle attached to a hand-held ¼-inch electric drill operated at high speed. The homogenate was centrifuged for 40 min at 18,000 × g. The supernatant was collected, and 4 M NaCl was added to it to yield a final concentration of 0.6 M NaCl. This solution was mixed gently by inversion and then incubated for 1 hr on ice to allow the formation of a precipitate. The precipitate was collected by centrifugation for 40 min at 18,000 × g. The precipitate was resuspended in a total of 50 ml of 25 mM Tris–HCl (pH 7.2) using a 40 ml Dounce homogenizer. Potassium–EDTA and potassium–EGTA were then added to final concentrations of 5 mM each, and 10% Triton X-100 (SurfactAmps, Pierce Chemical Company, Rockville, Illinois) was added to a final concentration of 1%. The resuspended pellets were homogenized gently to mix the solutions and to solubilize the membranous pellet; this was facilitated by briefly warming the Dounce by hand contact. The suspension was centrifuged for 40 min at 18,000 × g. The pellets, which had lost most of their previous volume and consisted primarily of myosin-V and actin, were combined and washed by resuspending them in a total of 50 ml of 25 mM Tris–HCl (pH 7.2). The washed pellets were centrifuged for 20 min at 18,000 × g. The pellets were resuspended in a total volume of 5–10 ml of 25 mM Tris–HCl, 600 mM NaCl, 5 mM $MgCl_2$, 2 mM EGTA, 10 mM ATP, 5 mM dithiothreitol (DTT) (pH 8.5) containing 25 μg/ml calmodulin. This solution was incubated on ice for 1 hr and then resuspended and incubated on ice for an additional hour. The solution was centrifuged for 10 min at 107,000 × g, and the supernatant was loaded onto a 1.5 × 100 cm S-500HR (Pharmacia, Uppsala, Sweden) gel filtration column preequilibrated in 25 mM Tris–HCl, 600 mM NaCl, 2 mM $MgCl_2$, 2 mM EGTA–sodium, 5 mM ATP, 5 mM DTT (pH 8.2). The column was operated at a flow rate of ~10 ml/hr, and 2.5 ml fractions were collected. The column profile was analyzed by SDS–polyacrylamide gel electrophoresis (SDS–PAGE) since the high absorbance of the ATP in the column buffer overshadowed the protein peaks. The myo-

sin-V-containing fractions were pooled so as to avoid contamination with the small myosin-II and fodrin peaks, which elute before myosin-V, and the tubulin and actin peaks, which elute after it. The pooled myosin-V was dialyzed a minimum of 6 hr against 4 l of Q-Sepharose buffer (20 mM triethanolamine, 250 mM NaCl, 1 mM EGTA-sodium, 5 mM DTT [pH 7.4] with HCl). The dialyzed myosin-V was loaded onto a 3 ml fast-flow Q-Sepharose (Pharmacia, Uppsala, Sweden) column preequilibrated with the same buffer. The column was then washed with 15–25 ml of Q-Sepharose buffer, and the myosin-V was eluted using a 250–750 mM NaCl gradient in column buffer with a total volume of 50 ml. Fractions (1 ml) were collected at a flow rate of no greater than 0.5 ml/min. Fractions were analyzed by SDS-PAGE, and those containing pure myosin-V were pooled. The myosin-V peak eluted at ~350–450 mM NaCl. To remove all traces of ATP, the myosin-V was dialyzed at least 1 day against several changes of buffer A (75 mM KCl, 20 mM imidazole-HCl, 2.5 mM $MgCl_2$, 1–10 mM DTT [pH 7.2]) containing either 0.1 or 1.0 mM EGTA. Pure myosin-V in this buffer that had been stored on ice for 1–2 weeks in the presence of freshly added DTT was enzymatically active and capable of movement in motility assays.

Proteins and Quantification

The extinction coefficient (at 280 nm for 1.0 mg/ml) of purified myosin-V was determined to be 1.04 using the 60°C enhanced BCA protein assay (Pierce Chemical Company, Rockford, Illinois) with bovine serum albumin as a standard. Similar extinction coefficients of 1.0 and 1.09 were obtained using the A_{205}/A_{280} methods described in Scopes (1987). Myosin-V was assumed to have a native molecular mass of 640 kd based on two 212,509 dalton heavy chains, four 16,837 dalton calmodulin light chains per heavy chain, and two additional light chains per heavy chain with apparent molecular masses of 23 and 17 kd. Actin was purified from chicken pectoralis muscle by the method of Spudich and Watt (1971). Skeletal muscle myosin-II was purified from chicken pectoralis muscle following the protocol of Kielley and Harrington (1959). Acanthamoeba castellani myosin-II was a gift of D. Kiehart (Duke University). Protein concentrations were calculated based on the following extinction coefficients at 280 nm for 1.0 mg/ml solutions: skeletal muscle myosin-II, 0.54; calmodulin in EGTA, 0.18; and actin, 1.09. Dilutions of bovine brain calmodulin (Calbiochem-Behring, San Diego, California), which has a deduced amino acid sequence identical to chicken calmodulin, were used as standards to quantitate the myosin-V light chains. Chicken skeletal muscle myosin-II was used as a standard to quantitate the myosin-V heavy chain. SDS-PAGE for the quantitation of the calmodulin light chains contained ~0.2 mM EDTA in the gel and electrophoresis buffers to force all of the calmodulin to migrate as a single band. A Hoeffer model 1650 scanning densitometer was used to integrate the adsorbance of the Coomassie blue-stained bands. The apparent molecular masses of the myosin-V light chains were determined by comparison with the molecular masses of the chicken muscle myosin-II light chains (25, 18, and 16 kd; Burridge and Bray, 1975) and calmodulin in the presence and absence of calcium (15 and 21 kd; Burgess et al., 1980).

Electron Microscopy

Purified myosin-V at ~60 μg/ml in Q-Sepharose buffer was visualized on mica as described in Heuser (1983). In brief, this involved adsorbing the molecules to a suspension of small flakes of mica and then pelleting the mica, washing it briefly in Q-Sepharose buffer, and quick freezing it as a slurry suspended in fresh Q-Sepharose buffer. The frozen slurry was then freeze fractured and deep etched to expose molecules on the surface of the mica flakes and replicated with 2 nm of evaporated platinum rotary deposited from 10° above the horizontal. Replicas were then cleaned in hydrofluoric acid to remove the mica, visualized in a standard transmission electron microscope operated at 100 kV, and photographed at 70,000× primary magnification with ± 10° tilt for stereo viewing. To stain myosin-V-decorated actin filaments negatively, mixtures of phalloidin-stabilized F-actin (5 μg/ml) and myosin-V (50–100 μg/ml) were incubated for 10 min at room temperature in buffer A, applied to parlodion-coated grids, and stained with 0.5% uranyl acetate.

ATPase and Motility Assays

ATPase assays were performed using a colorimetric method essentially as described in Conzelman and Mooseker (1987). Sliding filament assays were performed at ~24°C using the methods of Kron and Spudich (1986) as modified by Collins et al. (1990). Aliquots (20–100 μl) of myosin-V at 20–100 μg/ml in buffer A were flushed into motility chambers, and the myosin-V was allowed to adsorb to the nitrocellulose-coated coverslip for 2–15 min. Motility was observed in motility buffer, which consisted of buffer A plus 2 mM ATP, 200 μg/ml glucose oxidase, 100 μg/ml catalase, and 2.5 mg/ml glucose. In most experiments, actin filaments were present in the motility buffer at all times, and thus fresh filaments constantly settled onto the coverslip. Rates of filament movement were determined by measuring the starting and ending positions of ~30 filaments that had moved in approximately straight lines for several consecutive images. Nitella motility assays were performed at ~24°C essentially as described by Sheetz et al. (1986) using Covasphere beads (1 μm diameter; Duke Scientific, Palo Alto, California) that had been coated with myosin-V by incubating them with 9 vol of 200 μg/ml myosin-V in buffer A containing 1 mM EGTA and 0.25 mM phenylmethylsulfonyl fluoride for 2–5 min.

Miscellaneous

SDS-PAGE using 5%–16% linear gradient minigels was performed as in Conzelman and Mooseker (1987). Immunoblots with an affinity-purified antibody to chicken myosin-V (Espreafico et al., 1992) were used to estimate myosin-V abundance. The antibody to human platelet myosin was obtained from Biomedical Technologies Incorporated (Stoughton, Massachusetts). Western blots with the anti-calmodulin antibody 1F11 were performed on polyvinylidene difluoride membranes following essentially the transfer and fixation protocol reported in Hulen et al. (1991), except that alkaline phosphatase-conjugated secondary antibodies were used. Standard deviations for measurements are indicated by plus/minus values.

Acknowledgments

Correspondence should be addressed to R. E. C. We wish to thank Dr. Margaret Clarke for supplying the 1F11 monoclonal antibody to calmodulin. We also thank Dr. Matthew Heintzelman for his assistance with the dissections. Principal support for this work was provided by a Muscular Dystrophy Association grant to M. S. M. This work was also supported by an American Cancer Society postdoctoral grant to R. E. C., National Institutes of Health (NIH) grant GM-29647 to J. E. H., an NIH postdoctoral grant to J. S. W., a Coordenação de Aperfeiçoamento de Pessoal de Nível Superior grant to E. M. E., NIH grant NS-28695 to P. F., Fundação de Amparo a Pesquisa do Estado de São Paulo and Conselho Nacional de Desenvolvimento Científico e Tecnológico grants to R. E. L., and NIH grant DK-25387 to M. S. M.

Received May 12, 1993; revised July 27, 1993.

References

Andreasen, T. J., Luetje, C. W., Heideman, W., and Storm, D. R. (1983). Purification of a novel calmodulin binding protein from cerebral cortex membranes. Biochemistry *22*, 4615–4618.

Burgess, W. H., Jemiolo, D. K., and Kretsinger, R. H. (1980). Interaction of calcium and calmodulin in the presence of sodium dodecyl sulfate. Biochim. Biophys. Acta *623*, 257–270.

Burridge, K., and Bray, D. (1975). Purification and structural analysis of myosins from brain and other non-muscle tissues. J. Mol. Biol. *99*, 1–14.

Cheney, R. E., and Mooseker, M. S. (1992). Unconventional myosins. Curr. Opin. Cell Biol. *4*, 27–35.

Cheney, R. E., Riley, M. A., and Mooseker, M. S. (1993). Phylogenetic analysis of the myosin superfamily. Cell Motil. Cytoskel. *24*, 215–223.

Collins, K., Sellers, J. R., and Matsudaira, P. (1990). Calmodulin dissociation regulates brush border myosin I (110-kD-calmodulin) mechanochemical activity *in vitro*. J. Cell Biol. *110*, 1137–1147.

Conzelman, K. A., and Mooseker, M. S. (1987). The 110-kD protein-calmodulin complex of the intestinal brush border is an actin-activated Mg-ATPase. J. Cell Biol. *105*, 313–324.

Espindola, F. S., Espreafico, E. M., Coelho, M. V., Martins, A. R.,

Costa, F. R., Mooseker, M. S., and Larson, R. E. (1992). Biochemical and immunological characterization of p190–calmodulin complex from vertebrate brain: a novel calmodulin binding myosin. J. Cell Biol. *118*, 359–368.

Espreafico, E. M., Cheney, R. E., Matteoli, M., Nascimento, A. A. C., De Camilli, P. V., Larson, R. E., and Mooseker, M. S. (1992). Primary structure and localization of chicken brain myosin-V (p190), an unconventional myosin with calmodulin light chains. J. Cell Biol. *119*, 1541–1557.

Geiser, J. R., van Tuinen, D., Brockerhoff, S. E., Neff, M. M., and Davis, T. N. (1991). Can calmodulin function without binding calcium? Cell *65*, 949–959.

Goodson, H. V., and Spudich, J. A. (1993). Molecular evolution of the myosin family: relationships derived from comparisons of amino acid sequences. Proc. Natl. Acad. Sci. USA *90*, 659–663.

Halsall, D. J., and Hammer, J. A. (1990). A second isoform of chicken brush border myosin I contains a 29-residue inserted sequence that binds to calmodulin. FEBS Lett. *267*, 126–130.

Hayden, S. M., Wolenski, J. S., and Mooseker, M. S. (1990). Binding of brush border myosin I to phospholipid vesicles. J. Cell Biol. *111*, 443–451.

Heuser, J. E. (1983). Procedure for freeze-drying molecules absorbed to mica flakes. J. Mol. Biol. *169*, 155–195.

Hollenbeck, P. J. (1989). Distribution, abundance and subcellular localization of kinesin. J. Cell Biol. *108*, 2335–2342.

Hulen, D., Baron, A., Salisbury, J., and Clarke, M. (1991). Production and specificity of monoclonal antibodies against calmodulin from *Dictyostelium discoideum*. Cell Motil. Cytoskel. *18*, 113–122.

Ikura, M., Clore, G. M., Gronenborn, A. M., Zhu, G., Klee, C. B., and Bax, A. (1992). Solution structure of a calmodulin-target peptide by multidimensional NMR. Science *256*, 632–637.

Janson, L. W., Sellers, J. R., and Taylor, D. L. (1992). Actin-binding proteins regulate the work performed by myosin-II motors on single actin filaments. Cell Motil. Cytoskel. *22*, 274–280.

Johnston, G. C., Prendergast, J. A., and Singer, R. A. (1991). The *Saccharomyces cerevisiae MYO2* gene encodes an essential myosin for vectorial transport of vesicles. J. Cell Biol. *113*, 539–551.

Kakiuchi, S., Yasuda, S., Yamazaki, R., Teshima, Y., Kanda, K., Kakiuchi, R., and Subue, K. (1982). Quantitative determinations of calmodulin in the supernatant and particulate fractions of mammalian tissues. J. Biochem. *92*, 1041–1048.

Kendrick-Jones, J., and Scholey, J. M. (1981). Myosin-linked regulatory systems. J. Musc. Res. Cell Motil. *2*, 347–372.

Kielley, W. W., and Harrington, W. F. (1959). A model for the myosin molecule. Biochem. Biophys. Acta *41*, 401–421.

Knight, A. E., and Kendrick-Jones, J. (1993). A myosin-like protein from a higher plant. J. Mol. Biol. *231*, 148–154.

Kron, S. J., and Spudich, J. A. (1986). Fluorescent actin filaments move on myosin fixed to a glass surface. Proc. Natl. Acad. Sci. USA *83*, 6272–6276.

Kuznetsov, S. A., Langford, G. M., and Weiss, D. G. (1992). Actin-dependent organelle movement in squid axoplasm. Nature *356*, 722–725.

Larson, R. E., Pitta, D. E., and Ferro, J. A. (1988). A novel 190 kDa calmodulin-binding protein associated with brain actomyosin. Braz. J. Med. Biol. Res. *21*, 213–217.

Larson, R. E., Espindola, F. S., and Espreafico, E. M. (1990). Calmodulin-binding proteins and calcium/calmodulin-regulated enzyme activities associated with brain actomyosin. J. Neurochem. *54*, 1288–1294.

Lillie, S. H., and Brown, S. S. (1992). Suppresion of a myosin defect by a kinesin-related gene. Nature *356*, 358–361.

Mercer, J. A., Seperack, P. K., Strobel, M. C., Copeland, N. G., and Jenkins, N. A. (1991). Novel myosin heavy chain encoded by murine *dilute* coat colour locus. Nature *349*, 709–713. Erratum: Nature *352*, 547.

Mooseker, M. S., Wolenski, J. S., Coleman, T. R., Hayden, S. M., Cheney, R. E., Espreafico, E., Heintzelman, M. B., and Peterson, M. D. (1991). Structural and functional dissection of a membrane-bound mechanoenzyme: brush border myosin I. Curr. Top. Membr. *38*, 31–55.

Plancke, Y. D., and Lazarides, E. (1983). Evidence for a phosphorylated form of calmodulin in chicken brain and muscle. Mol. Cell. Biol. *3*, 1412–1420.

Rayment, I., Rypniewski, W. R., Schmidt-Bäse, K., Smith, R., Tomchick, D. R., Benning, M. M., Winkelmann, D. A., Wesenberg, G., and Holden, H. M. (1993). Three-dimensional structure of myosin subfragment-1: a molecular motor. Science *261*, 50–58.

Ruppert, C., Kroschewski, R., and Bähler, M. (1993). Identification, characterization and cloning of *myr1*, a mammalian myosin-I. J. Cell Biol. *120*, 1393–1403.

Scopes, R. K. (1987). Protein Purification, Principles and Practice, Second Edition (New York:Springer-Verlag).

Sheetz, M. P., Block, S. M., and Spudich, J. A. (1986). Myosin movement *in vitro*: quantitative assay using oriented actin cables from Nitella. Meth. Enzymol. *134*, 531–543.

Silvers, W. K. (1979). *Dilute* and *Leaden*, the *p*-locus, *ruby-eye* and *ruby-eye-2*. In Coat Colors of Mice: A Model for Mammalian Gene Action and Interaction, W. K. Silvers, ed. (New York: Springer-Verlag), pp. 83–104.

Spudich, J. A., and Watt, S. (1971). Regulation of skeletal muscle contraction. I. Biochemical studies of interaction of the tropomyosin–troponin complex with actin and the proteolytic fragments of myosin. J. Biol. Chem. *246*, 4866–4871.

Swanljung-Collins, H., and Collins, J. H. (1991). Ca^{2+} stimulates the Mg^{2+}–ATPase activity of brush border myosin I with three or four calmodulin light chains but inhibits with less than two bound. J. Biol. Chem. *266*, 1312–1319.

Takiguchi, K., Hayashi, H., Kurimoto, E., and Higashi-Fujime, S. (1990). *In vitro* motility of skeletal muscle myosin and its proteolytic fragments. J. Biochem. *107*, 671–679.

Toyoshima, Y. Y., Kron, S. J., and Spudich, J. A. (1990). The myosin step size: measurement of the unit displacement per ATP hydrolyzed in an *in vitro* assay. Proc. Natl. Acad. Sci. USA *87*, 7130–7134.

Umemoto, S., and Sellers, J. R. (1990). Characterization of *in vitro* motility assays using smooth muscle and cytoplasmic myosins. J. Biol. Chem. *265*, 14864–14869.

Wang, K. K. W., Villalobo, A., and Roufogalis, B. D. (1989). Calmodulin-binding proteins as calpain substrates. Biochem. J. *262*, 693–706.

Wolenski, J. S., Cheney, R. E., Forscher, P. A., and Mooseker, M. S. (1993a). *In vitro* motilities of the unconventional myosins, brush border myosin-I and chick brain myosin-V, exhibit assay-dependent differences in velocity. J. Exp. Zool., in press.

Wolenski, J. S., Hayden, S. M., Forscher, P., and Mooseker, M. S. (1993b). Calcium–calmodulin and regulation of brush border myosin-I MgATPase and mechanochemistry. J. Cell Biol. *122*, 613–622.